Time-Temperature-Water Absorption Dependent Fatigue Strength of Plain-Woven CFRP Laminates

Yasushi Miyano*, Masayuki Nakada*, Naoyuki Sekine** and Jun Ichimura**

* *Materials System Research Laboratory, Kanazawa Institute of Technology, 3-1 Yatsukaho Matto, Ishikawa 924-0838, Japan*
** *Graduate School, Kanazawa Institute of Technology, 7-1 Ohgigaoka Nonoichi, Ishikawa 921-8501, Japan*

ABSTRACT

This paper is concerned with the influence of water absorption on the time-temperature dependent flexural strength of plain-woven CFRP laminates for advanced marine use. The CFRP laminates consist of plain-woven PAN-based carbon fiber and vinylester resin, which were treated under the three conditions of Dry, Wet (0.6%; saturated) and Wet+Dry after molding. Three-point bending constant-strain rate (CSR) and fatigue tests for these three types of specimen were carried out under various loading-rates and temperatures. The flexural CSR and fatigue strengths depend remarkably on the water absorption as well as time and temperature. The applicability of time-temperatures-water absorption superposition principle as well as time-temperatures superposition principle was experimentally confirmed for these strengths, therefore, the master curves for fatigue strengths can be obtained. It is clear from the master curves that the fatigue strength decreases remarkably with time to failure, temperature and water absorption; however, it scarcely decreases with number of cycles to failure. Concretely, the flexural fatigue strength decreases by 40% during 50 years, 27% by 0.6% water absorption and only 5% by 10^5 load cycles.

1. INTRODUCTION

Recently carbon fiber reinforced plastics (CFRP) have been used for the primary structures of airplanes, ships, spacecrafts etc., in high reliability should be maintained during long-term operation. Therefore, it is extremely desirable that an accelerated testing methodology for the long-term life prediction of composite structures exposed in the actual environments of temperature, water, etc., should be established.

The mechanical behavior of polymer resins exhibits time and temperature dependence, called viscoelastic behavior, not only above the glass transition temperature T_g but also below T_g /1-8/. Furthermore, the viscoelastic behavior of polymer resins also depends on the water absorption /9-12/. Thus, it can be presumed that the mechanical behavior of polymer composites significantly depends on the water absorption as well as time and temperature.

This paper is concerned with the influence of water absorption on the time-temperature dependent flexural strength of plain-woven CFRP laminates for advanced marine use. The CFRP laminates consist of plain-woven PAN-based carbon fiber and vinylester resin, which were treated under the three conditions of Dry, Wet (0.6%; saturated) and Wet+Dry after molding. Three-point bending constant-strain rate (CSR) and fatigue tests for these three types of specimen were carried out under various loading-rates and temperatures. The influence of water absorption on time-temperature dependent flexural CSR and fatigue strengths is evaluated, and the applicability of time-temperatures-water absorption superposition principle (TTWSP) as well as time-temperatures superposition principle (TTSP) is discussed.

2. EXPERIMENTAL PROCEDURE

2.1 Preparation of specimens

The CFRP laminates which consist of plain-woven carbon fiber (Toray, T300) and vinylester resin (Dow, 411-350) were formed by resin transfer molding (RTM). Cure condition for this CFRP laminate was over 24 hours at room temperature. The fiber volume fraction was approximately 51%. The thickness of the laminates was 2mm.

The test specimens for creep, CSR, and fatigue tests were cut from this CFRP laminate. These test specimens were treated under the three conditions of Dry, Wet and Wet+Dry as shown in Table 1. The Dry specimens were obtained by holding the cured specimen in the oven at 150°C for 2 hours. The Wet specimens were obtained by soaking the Dry specimens in hot water at 95°C for 120 hours. The Wet+Dry specimens were obtained by dehydrating the Wet specimens in the oven at 150°C for 2 hours.

Table 1

Treated conditions for Dry, Wet, and Wet+Dry specimens

	Water content	In oven		In water		In oven
Dry	0%	150°C x 2h		-		-
Wet	0.6%	150°C x 2h	+	95°C x 120h		-
Wet + Dry	0%	150°C x 2h	+	95°C x 120h	+	150°C x 2h

2.2 Experimental procedures

To confirm the applicability of TTSP and TTWSP for the viscoelastic properties of this CFRP laminate, the three-point bending creep tests for Dry, Wet and Wet+Dry specimens (length l=60mm, width b=25mm, and thickness h=2.0mm) were carried out under various temperatures using a creep testing machine with a constant temperature chamber. The creep compliance D_c was calculated from the deflection δ at the center of specimen using the following equation:

$$D_c = \frac{4bh^3\delta}{PL^3} \tag{1}$$

where P is the applied load. L is the span (L=50mm).

The three-point bending CSR and fatigue tests for Dry, Wet and Wet+Dry specimens (l=80mm, b=15mm, h=2.0mm) were carried out under various loading rates and temperatures. The span is L=60mm. The CSR tests were conducted at three loading-rates V=0.02, 2, 200 mm/min and several constant temperatures T using an universal testing machine with a temperature chamber. The fatigue tests were conducted under several constant temperatures T for two loading frequencies f=2Hz and 0.02Hz, and a stress ratio (minimum stress/maximum stress) R=0.05 using an electro-hydraulic servo testing machine with a temperature chamber. The flexural stress σ is calculated from applied load P by

$$\sigma = \frac{3PL}{2bh^2}. \tag{2}$$

In order to prevent the dryness of Wet specimen during creep, CSR, and fatigue tests, the Wet specimens were wrapped in a vinyl bag with distilled water.

3. RESULTS AND DISCUSSION

3.1 Creep compliance

The left side of Fig. 1 shows the creep compliance D_c versus testing time t at various temperatures T for Dry, Wet and Wet+Dry specimens. The master curves of D_c versus the reduced time t' were constructed by shifting D_c at various constant temperatures along the log scale of t. Since the smooth master curve of D_c for each specimen can be obtained as shown in the right side of each graph, the TTSP is applicable for each D_c. From Fig.1 (b) and (c), it is clear that D_c increases with water absorption and returns perfectly to that of Dry specimen by re-drying after water absorption.

The time-temperature shift factor $a_{T0}(T)$ at a reference temperature T_0 is defined by

$$\log a_{T_0}(T) = \log t - \log t' \tag{3}$$

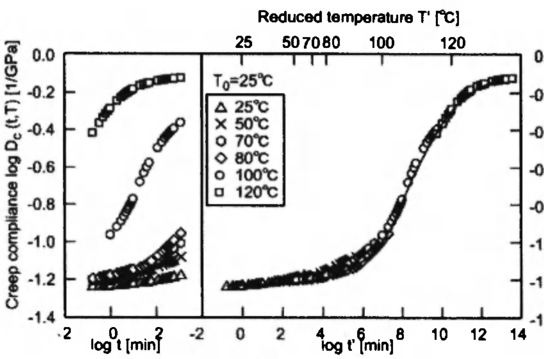

(a) Dry specimen

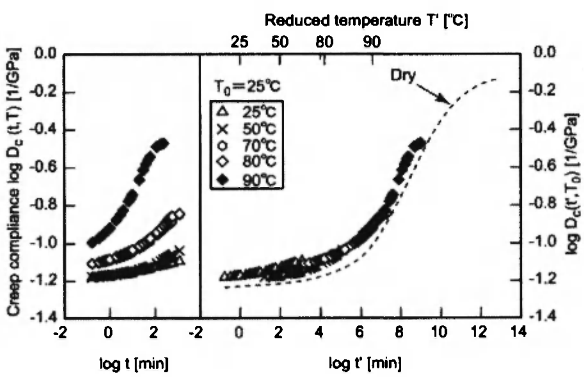

(b) Wet specimen

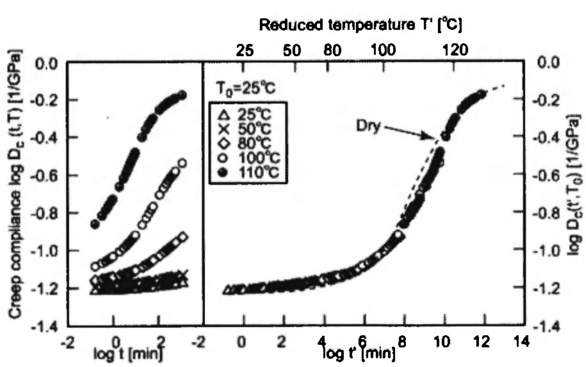

(c) Wet+Dry specimen

Fig. 1: Master curves of creep compliance

The $a_{T_0}(T)$ for each D_c obtained experimentally in Fig. 1 are plotted in Fig. 2. The $a_{T_0}(T)$ for each D_c are described by two Arrhenius' equations with different activation energies ΔH:

$$\log a_{T_0}(T) = \frac{\Delta H}{2.303R}\left(\frac{1}{T} - \frac{1}{T_0}\right) \tag{4}$$

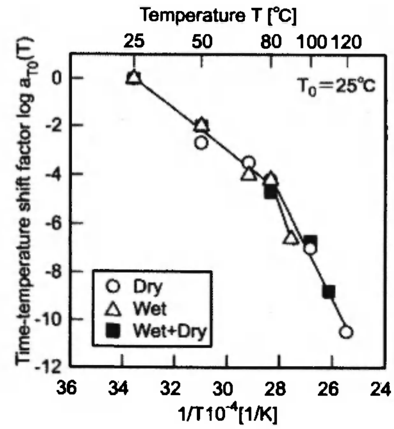

Fig. 2: Time-temperature shift factors of creep compliance

where R is the gas constant $8.314\text{x}10^{-3}$ [kJ/(K·mol)].

From Fig.2, it is clear that the knee point temperature of $a_{T_0}(T)$ decreases with water absorption and returns perfectly to that for Dry specimen by re-drying after water absorption.

The left side of Fig. 3 shows the master curves of D_c for Dry, Wet and Wet+Dry specimens. The grand-master curve for D_c versus the reduced-reduced time t'' can be constructed by shifting the master curve D_c for Wet specimen along the log scale of t' so that they overlap on D_c at the reference water content W_0=0% (Dry specimen) to form a single smooth grand-master curve as shown in the right side of this figure. Therefore, the TTWSP is applicable for D_c.

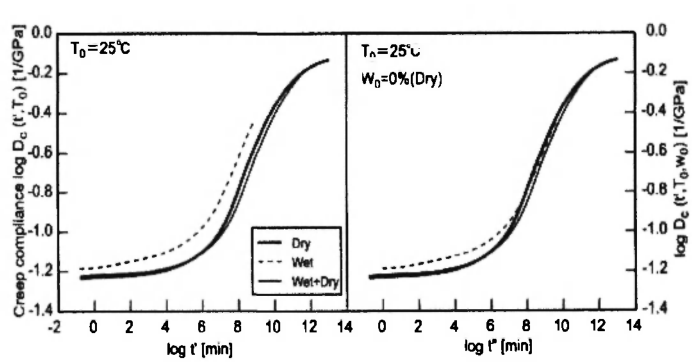

Fig. 3: Grand-master curve of creep compliance

The time-temperature-water absorption shift factor $a_{T_0,W_0}(T, W)$ at a reference water content W_0 is defined by

$$\log a_{T_0,W_0}(T,W) = \log t - \log t' - \log t' \quad (5)$$

The $a_{T_0,W_0}(T, W)$ obtained experimentally from Fig. 3 were plotted in Fig. 4.

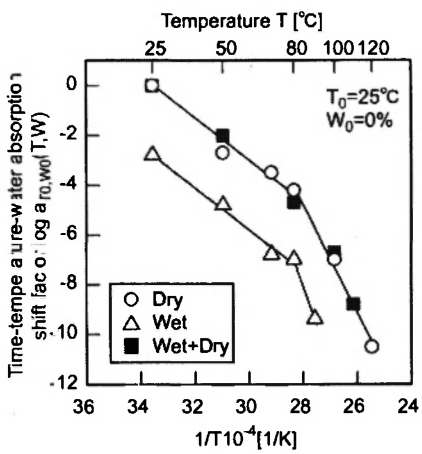

Fig. 4: Time-temperature-water absorption shift factor of creep compliance

3.2 Flexural CSR strength

The left side of Fig. 5 shows the flexural CSR strength σ_s versus time to failure t_s at various temperatures T for Dry, Wet, Wet+Dry specimens, where t_s is the time period from initial loading to maximum load during testing. The master curves of σ_s versus the reduced time to failure t_s' were constructed by shifting σ_s at various constant temperatures along the log scale of t_s using the same shift factors for D_c as shown in Fig.3. Since the smooth master curve of σ_s for each specimen can be obtained as shown in the right side of each graph, the TTSP for D_c is also applicable for each σ_s. From Fig.5 (b) and (c), it is cleared that σ_s decreases with water absorption and returns to that of Dry specimen by re-drying after water absorption.

The left side of Fig.6 shows the master curves of σ_s for Dry and Wet specimens. A smooth grand-master curve of σ_s was obtained by shifting the master curve of σ_s for Wet specimen along the log scale of t_s' using the same shift factors for creep compliance D_c as shown in Fig. 4. Therefore, the TTWSP for D_c also holds for σ_s.

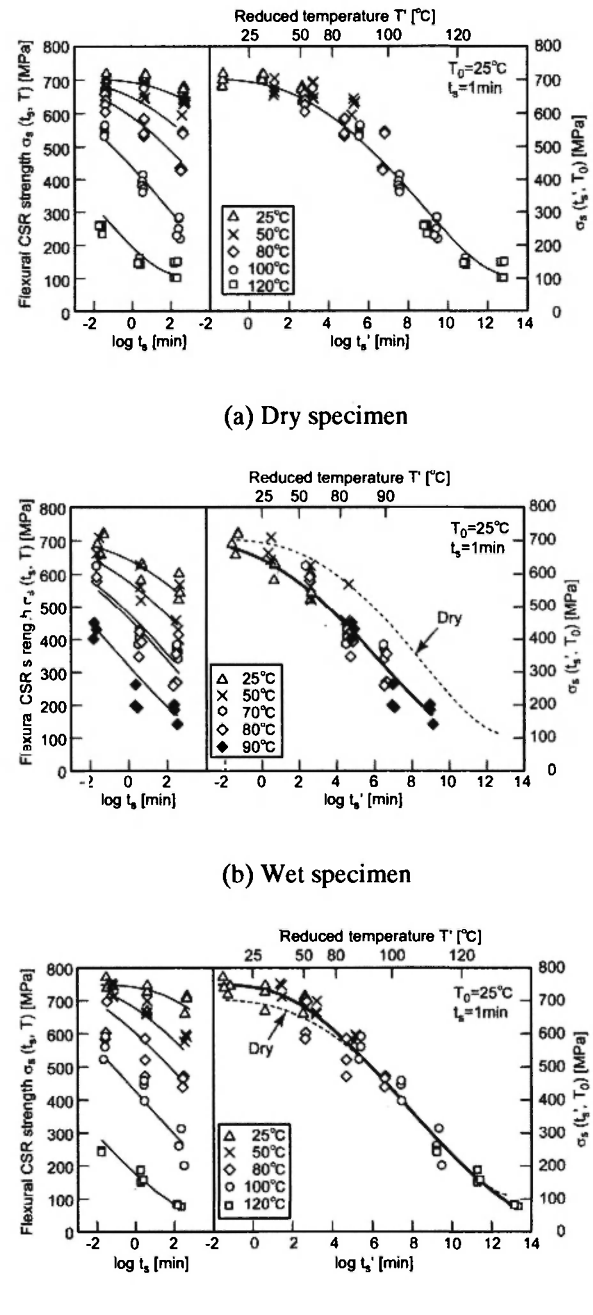

(a) Dry specimen

(b) Wet specimen

(c) Wet+Dry specimen

Fig. 5: Master curves of flexural CSR strength

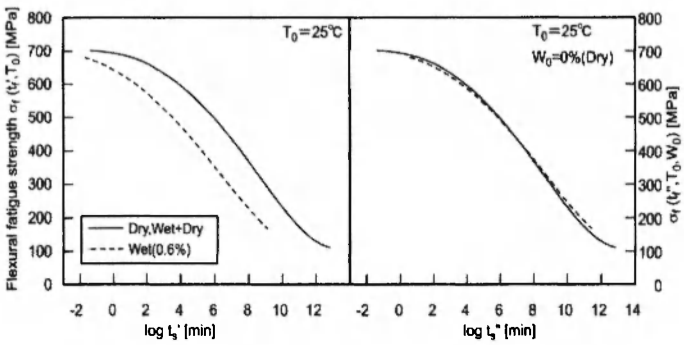

Fig. 6: Grand-master curve of flexural CSR strength

3.3 Flexural fatigue strength

To describe the master curve of flexural fatigue strength, σ_f, we need the reduced frequency $f\,'$ in addition to the reduced time to failure t_f', each defined by

$$f' = f \cdot a_{T_0}(T)\ , \quad t_f' = \frac{t_f}{a_{T_0}(T)} = \frac{N_f}{f'} \tag{6}$$

where N_f is the number of cycles to failure.

The σ_f versus N_f at frequency f=2Hz for Dry, Wet, and Wet+Dry specimens are shown in Fig. 7 where σ_f at N_f=1/2 is represented by σ_s at $t_s=(2f)^{-1}$. In the upper figure of Fig. 8, σ_f versus t_f' curves of Dry specimen for several $f\,'$ at T_0 are depicted by solid lines, which are obtained by converting N_f on Fig. 7 (a) into t_f' using Eq. 6 and the shift factor of CSR strength for Dry specimen. The master curves of σ_f for fixed N_f indicated by solid lines in the lower figure are constructed by connecting the points of the same N_f on the curves of each $f\,'$ indicated by dotted lines in this figure.

Figure 9 shows the master curves of σ_f for Wet and Wet+Dry specimens which are obtained from the σ_f-N_f curves at f=2Hz for Wet and Wet+Dry specimens as shown in Fig. 7 (b) and (c) using the shift factor of CSR strength for Wet and Wet+Dry specimens, respectively. From this figure, it is clear that the σ_f decreases with water absorption and returns to that of Dry specimen by re-drying after water absorption.

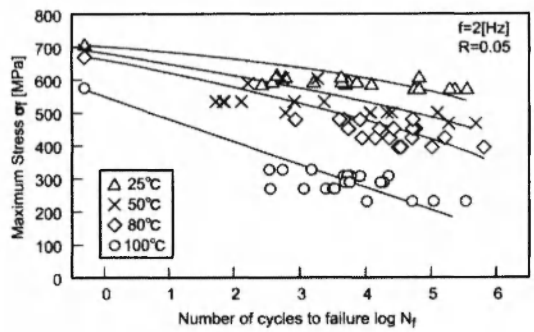

(a) Dry specimen

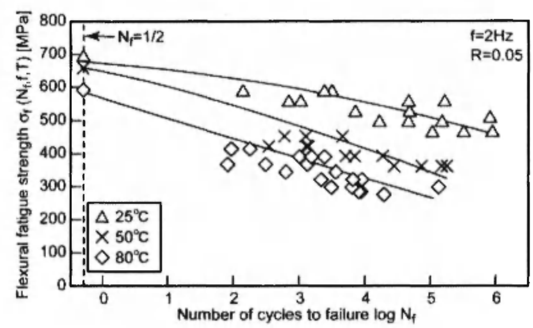

(b) Wet specimen

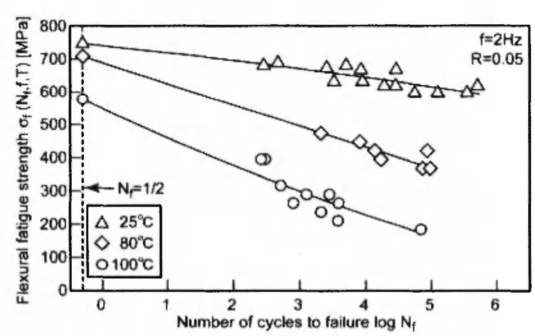

Wet + Dry specimen

Fig. 7: Flexural fatigue strength versus number of cycles to failure at frequency 2Hz

In order to confirm the applicability of TTSP for fatigue strength of Dry, Wet, Wet+Dry specimens, we predicted the σ_f-N_f curves at f=0.02Hz and compared them with the test results as shown in Fig. 10. The predicted σ_f from fatigue master curves agree well with experimental ones, therefore, the TTSP for CSR strength also holds for fatigue strength for Dry, Wet, and Wet+Dry specimens, respectively.

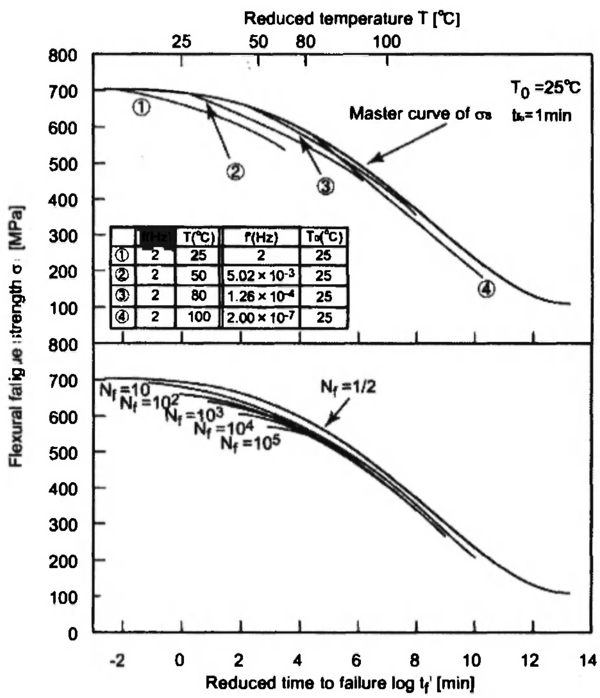

Fig. 8: Master curves of flexural fatigue strength for Dry specimen

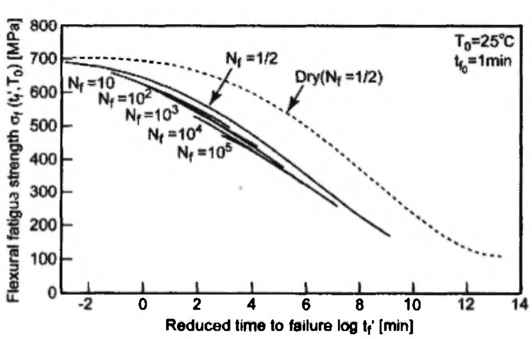

(a) Wet specimen

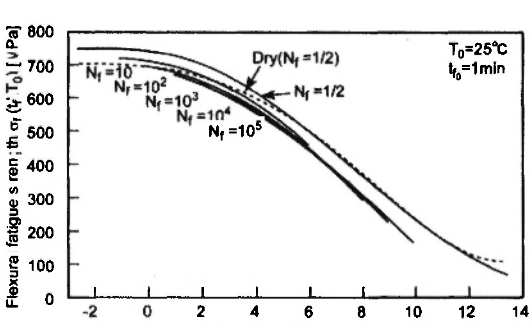

(b) Wet+Dry specimen

Fig. 9: Master curves of flexural fatigue strength

Figure 11 shows the master curves of σ_f at N_f=1/2 and 10^5 for Dry and Wet specimens. These master curves can be superimposed by shifting the master curves for Wet specimen along the log scale of t_f' using the shift factor $a_{T_0,W_0}(T,W)$ for D_c in Fig.4 as shown in Fig.12. Therefore, the TTWSP for D_c also holds for σ_f.

It is clear from the fatigue master curves in Fig. 13 that the σ_f decreases remarkably with time to failure, temperature and water absorption; however, it scarcely decreases with N_f. Concretely, the σ_f decreases in 40% during 50 years, 27% by 0.6% water absorption and only 5% by 10^5 load cycles.

Finally, we compared the fatigue strength of CFRP laminates T300/VE for advanced marine use with that of GFRP laminates E-glass/VE for conventional marine use. The fatigue strength of Dry specimen for T300/VE scarcely decreases with increasing the number of cycles to failure N_f, although that for E-glass/VE decreases strongly with increasing N_f, as shown in Fig.14.

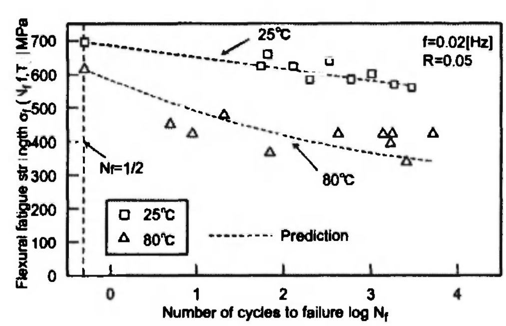

(a) Dry specimen

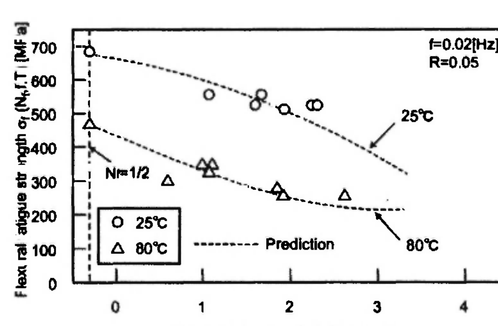

(b) Wet specimen

Fig. 10 (cont'd)

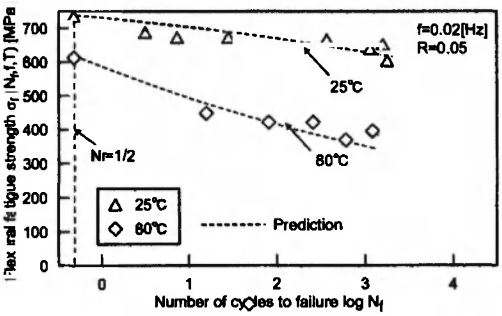

(c) Wet+Dry specimen

Fig. 10: Prediction of flexural fatigue strength at frequency 0.02Hz

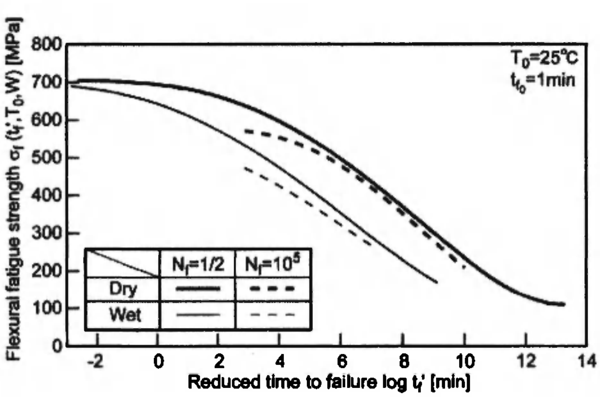

Fig. 11: Master curves of flexural fatigue strength for Dry and Wet specimens

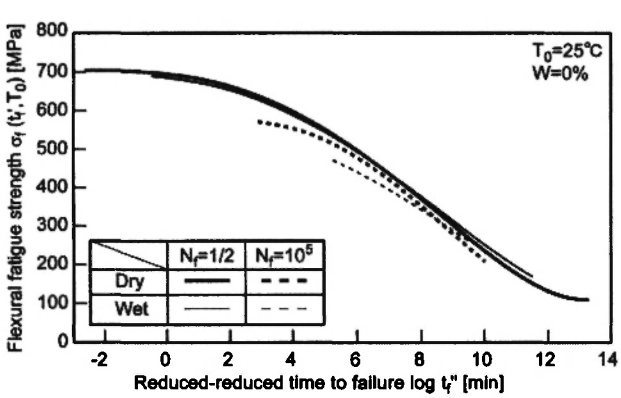

Fig. 12: Grand-master curve of flexural fatigue strength

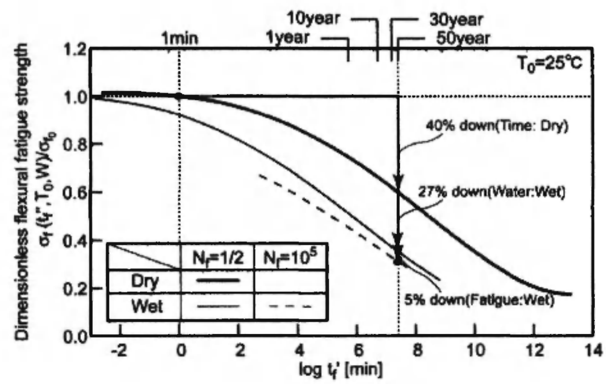

Fig. 13: Fatigue life prediction under water absorption condition

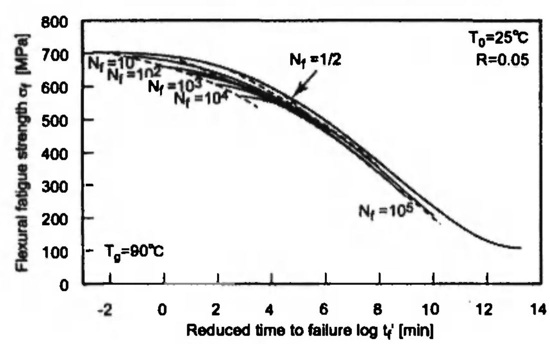

(a) CF/VE laminate

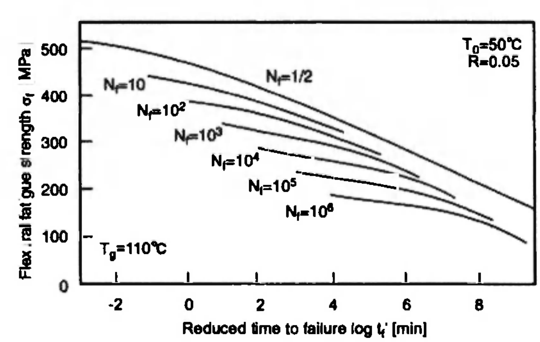

(b) GF/VE laminate

Fig. 14: Comparison of master curves of flexural fatigue strength CF/VE and GF/VE laminates

4. CONCLUSION

This paper is concerned with the influence of water absorption on the time-temperature dependent flexural strength of plain-woven CFRP laminates for advanced marine use. The CFRP laminates consist of plain-woven PAN-based carbon fiber and vinylester resin, which were treated under the three conditions of Dry, Wet (0.6%; saturated) and Wet+Dry after molding. Three-point bending CSR and fatigue tests for these three types of specimen were carried out under various loading-rates and temperatures. The flexural CSR and fatigue strengths depend remarkably on the water absorption as well as time and temperature. The applicability of TTWSP as well as TTSP was experimentally confirmed for the flexural CSR and fatigue strengths, the master curves for these strengths can be obtained. It is clear from these master curves that the flexural fatigue strength decreases remarkably with time to failure; temperature and water absorption, however scarcely decrease with number of cycles to failure N_f.

ACKNOWLEDGEMENTS

The authors thank the Office of Naval Research for supporting this work through an ONR award (N000140110949) with Dr. Yapa Rajapakse as the ONR Program Officer. The authors thank Professor Richard Christensen at Stanford University as the consultant of this project and Toray Industries, Inc. as the supplier of CFRP laminates.

REFERENCES

1. J. Aboudi and G. Cederbaum, *Composite Structures*, **12**, 243-256 (1989).
2. J.L. Sullivan, *Composite Science and Technology*, **39**, 207-232 (1990).
3. T. Gates, *Experimental Mechanics*, **68**, 73 (1992).
4. Y. Miyano, M. Kanemitsu, T. Kunio and H. Kuhn, *J. Composite Materials*, **20**, 520-538 (1986).
5. Y. Miyano, M.K. McMurray, J. Enyama and M. Nakada, *J. Composite Materials*, **28**, 1250-1260 (1994).
6. Y. Miyano, M.K. McMurray, N. Kitade, M. Nakada and M. Mohri, *Advanced Composite Materials*, **4**, 87-99 (1994).
7. Y. Miyano, M. Nakada and M.K. McMurray, *J. Composite Materials*, **29**, 1808-1822 (1995).
8. Y. Miyano, M. Nakada, M.K. McMurray and R. Muki, *J. Composite Materials*, **31**, 619-638 (1997).
9. C.H. Shen and G.S. Springer, *J. Composite Materials*, **10**, 2-20 (1976).
10. K.G. Kibler, *AGRD Conference Proceedings*, 8-1, (1980).
11. S. Neumann and G. Marom, *Polymer Composites*, **6**, 9-12 (1985).
12. R. Selzer and K. Friedrich, *Composites Part A*, **28A**, 595-604 (1997).